MCP Papers in Press. Published on August 22, 2018 as Manuscript RA118.000704

Comparative secretome analyses of primary murine white and brown adipocytes reveal novel adipokines

Asrar Ali Khan[1,2,3,4], Jenny Hansson[5,6], Peter Weber[1,2,3,4,7], Sophia Foehr[5,8], Jeroen Krijgsveld[5,8], Stephan Herzig[1,2,3,4], Marcel Scheideler[1,2,3,4,*]

[1] Institute for Diabetes and Cancer (IDC), Helmholtz Zentrum München, Neuherberg, Germany

[2] Joint Heidelberg-IDC Translational Diabetes Program, Heidelberg University Hospital, Heidelberg, Germany

[3] Molecular Metabolic Control, Medical Faculty, Technical University Munich, Germany

[4] German Center for Diabetes Research (DZD), Neuherberg, Germany

[5] Genome Biology Unit, European Molecular Biology Laboratory (EMBL), Heidelberg, Germany

[6] Current address: Division of Molecular Hematology, Lund Stem Cell Center, Lund University, Lund, Sweden

[7] Radiation Cytogenetics, Helmholtz Zentrum München, Neuherberg, Germany

[8] Proteomics of Stem Cells and Cancer, German Cancer Research Center (DKFZ), Heidelberg, Germany

[*] Correspondence should be addressed to: Marcel Scheideler, Phone: +49-89-3187-1047, Email: marcel.scheideler@helmholtz-muenchen.de

Running title: Comparative secretome analysis of white and brown adipocytes

Abbreviations

AHA – L-azidohomoalanine

BA – brown adipocytes

BAT – brown adipose tissue

ECM – extracellular matrix

GO – Gene Ontology

pSILAC – pulsed stable isotope labeling with amino acids in cell culture

NE – norepinephrine

SVF – stroma vascular fraction

WA – white adipocytes

WAT – white adipose tissue

Summary

The adipose organ, including white and brown adipose tissues, is an important player in systemic energy homeostasis, storing excess energy in form of lipids while releasing energy upon various energy demands. Recent studies have demonstrated that white and brown adipocytes also function as endocrine cells and regulate systemic metabolism by secreting factors that act locally and systemically. However, a comparative proteomic analysis of secreted factors from white and brown adipocytes and their responsiveness to adrenergic stimulation has not been reported yet. Therefore, we studied and compared the secretome of white and brown adipocytes, with and without norepinephrine (NE) stimulation. Our results reveal that carbohydrate metabolism-regulating proteins are preferably secreted from white adipocytes, while brown adipocytes predominantly secrete a large variety of proteins. Upon NE stimulation, an increased secretion of known adipokines is favored by white adipocytes while brown adipocytes secreted higher amounts of novel adipokines. Furthermore, the secretory response between NE-stimulated and basal state was multifaceted addressing lipid and glucose metabolism, adipogenesis and anti-oxidative reactions. Intriguingly, NE stimulation drastically changed the secretome in brown adipocytes. In conclusion, our study provides a comprehensive catalogue of novel adipokine candidates secreted from white and brown adipocytes with many of them responsive to NE. Given the beneficial effects of brown adipose tissue activation on its endocrine function and systemic metabolism, this study provides an archive of novel batokine candidates and biomarkers for activated brown adipose tissue.

Keywords

Secretome, white adipocytes, brown adipocytes, murine SVF cells, adrenergic stimulation

Introduction

The adipose organ has an important role in regulating fatty acid and glucose metabolism for whole-body energy homeostasis. In mammals, this is mediated by two distinct types of adipose tissues: white adipose tissue (WAT) which is specialized in the storage of lipids upon energy surplus and in lipid release upon energy deprivation, and brown adipose tissue (BAT) which is able to dissipate energy in the form of heat, called non-shivering thermogenesis, upon adrenergic stimulation. Both tissue types are essential for metabolic health, as disruption of normal WAT function leads to insulin resistance (1, 2), while the activation of BAT increases glucose uptake, thus leading to decreased blood glucose levels, improved insulin sensitivity and weight loss (3, 4).

WAT is also widely recognized as an endocrine organ owing to the discovery of several adipose tissue-specific secreted proteins called adipokines. These include leptin that controls satiety and body weight, adiponectin that increases insulin sensitivity, and resistin that contributes to insulin resistance and that has a pro-inflammatory effect (5-7). However, BAT, unlike its white counterpart, has just emerged as an endocrine tissue (8). Interestingly, mice completely lacking BAT became obese while mice only deficient in UCP1 became cold-sensitive but not obese (9, 10). These studies suggest that BAT can affect whole-body energy homeostasis by UCP1-dependent and independent mechanisms involving ‘brown adipokines’ or ‘batokines’. Indeed, recent studies in mice and rats have identified the first brown adipokine candidates with autocrine, paracrine and endocrine functions, including vascular endothelial growth factor-A (VEGF-A), insulin-like growth factor I (IGF-I), fibroblast growth factor-2 (FGF2), FGF21, neuregulin 4 (NRG4), triiodothyronine (T3), interleukin 6 (IL-6) and bone morphogenetic protein 8b (BMP8b) (11). These factors have various functions like promoting angiogenesis (VEGF-A) or increasing sensitivity to adrenergic stimulation (BMP8b) (11). However, a comprehensive and comparative proteomic analysis in primary murine white and brown adipocytes, including stimulation with norepinephrine (NE), a catecholamine that triggers essential physiological responses in adipose tissues, has not been reported so far.

Therefore, in this study, we investigated the secretome of stroma-vascular fraction (SVF)-derived murine white and brown adipocytes by using mass spectrometry combined with click-chemistry and pulsed stable isotope labeling with amino acids in cell culture (pSILAC). We conducted three comparative analyses: the first two compared the secretome of white and brown adipocytes without and with NE treatment, respectively, while the third experiment compared brown adipocytes with and without NE stimulation. We found that white adipocytes predominantly secrete carbohydrate metabolism-regulating proteins, while brown adipocytes

preferentially secrete integrin signaling proteins. With NE stimulation, this secretory signature in white adipocytes changed to more secreted proteins involved in lipid metabolism, while in brown adipocytes the secretory profile shifted more to specific proteins with anti-inflammatory properties. When comparing this NE-stimulated to the unstimulated (basal) state, the secretory profile between white and brown adipocytes became complex targeting lipolysis, glucose uptake, browning of white adipocytes and protection against oxidative stress. Moreover, in brown adipocytes, NE stimulation broadly and significantly altered the adipocyte secretome. In conclusion, our study provides a comprehensive insight into the secretome of white and brown adipocytes with numerous novel adipokine candidates, in part also responsive to NE.

Experimental Procedures

Isolation, culturing and adipocyte differentiation of murine SVF cells

Mouse primary preadipocytes were isolated from 8 weeks old male C57BL/6J mice (Charles River). The inguinal WAT and interscapular BAT were excised and placed in ice-cold 1X D-PBS (Gibco). Next, the organs were cleaned by removing the lymph nodes from WAT and residual WAT from BAT. Both adipose tissues were minced and digested in collagenase. WAT was digested in DMEM-based collagenase solution consisting of 1.5 mg/ml collagenase II (Sigma) and 0.5% bovine serum albumin (Sigma) while BAT was digested with additional 15 mM HEPES (Gibco), 3.2 mM $CaCl_2$ and 10% FBS at 37°C, centrifuged at 100 rpm until no tissue clumps were visible (less than an hour). The digestion solution was centrifuged at 1,000 rpm for 5 minutes and the pellet was resuspended in DMEM growth media (10% FBS, 1% Pen/Strep) and passed through a 70 µm nylon filter (Fisher Scientific). The cells were plated on 12 well plates, and differentiation was started after the cells reached confluency by the addition of 1 mg/ml insulin, 0.5 mM 3-isobutyl-1-methylxanthine (IBMX), 0.25 mM dexa-methasone, and 1/1,000 volume ABP (50 mg/ml L-ascorbate, 1 mM biotin, 17 mM pantothenate) in high (4.5 g/l) glucose DMEM containing 10% FCS and 1% Pen/Strep. 1 nM of triiodothyronine (T3) was added additionally for differentiating brown preadipocytes. The same media was added on day 2 and only insulin and ABP (T3 for brown adipocytes) were added on day 4. Starting day 6 of differentiation DMEM growth media (10% FBS, 1% Pen/Strep) was added to the cells.

Measurement of cell death

The cytotoxic effect of AHA supplemented media on primary adipocytes was measured using the Cytotoxicity Detection Kit (LDH) (Roche) based on the manufacturer's instructions. Fresh growth media was taken as

blank and adipocytes treated with 1% Triton X-100 (Sigma) was the positive control. The percentage of cell death or LDH release was depicted as % LDH compared to the positive control (100 % cell death).

Measurement leptin and resistin concentrations in cellular supernatant using MILLIPLEX® MAP mouse metabolic hormone panel

The MILLIPLEX® MAP Mouse Metabolic Hormone panel (Cat. # MMHMAG-44K) was used with the Luminex xMAP® platform (MAGPIX®) to detect leptin and resistin in tissue culture supernatant from primary adipocytes. The immunoassay procedure was carried out according to the manufacturer's instructions and was analyzed on the MAGPIX® with the xPONENT software. The Median Fluorescent Intensity (MFI) data was analyzed using a 5-parameter logistic method for calculating the concentrations of leptin and resistin in the samples.

Experimental design and statistical rationale

We performed the comparative secretome studies by combining L-azidohomoalanine (AHA) and pSILAC labeling (12). This involved concomitant pulse-labeling of the cell population with AHA, an azide-bearing analog of methionine, and stable isotope-labeled amino acids. AHA allows the enrichment (by selective and covalent capture) of newly synthesized AHA-containing proteins using an alkyne-activated resin via click-chemistry. SILAC was then used to quantitatively compare secretome composition of cells between two different conditions. The resultant secreted proteome obtained by the combination of these two techniques was analyzed using mass spectrometry (Figure 1).

Specifically, to deplete cells of methionine, lysine and arginine, the cells were incubated for 30 min in depletion medium (DMEM non-GMP formulation without methionine, arginine and lysine; GIBCO) with 10% FBS (GIBCO) before incubation in the same medium supplemented with 0.1 mM l-AHA (AnaSpec, Inc) and either 84 µg/ml [13C6,15N4] l-arginine and 146 µg/ml [13C6,15N2]l-lysine or 84 µg/ml [13C6]l-arginine and 146 µg/ml [4,4,5,5-D4]l-lysine (Cambridge Isotope Laboratories, Inc). The cells were either stimulated for 24 hours with 0.5 µM norepinephrine (Sigma) or not, along with the labeled amino acid media. The supernatants were collected from a row of 4 wells of a 12 well plate and pooled together as one replicate. There were three replicates for each analysis and the third replicate in each analysis was reciprocally labeled compared to the first two. Collected supernatant samples were centrifuged (5 min at 1,000 g), cOmplete™ EDTAfree protease inhibitor (Roche) was added and the mixture was frozen at -80°C. DNA was extracted from the cells left behind on the plate and used to normalize the mixing of the collected media before the enrichment.

Enrichment of newly synthesized proteins and on-bead digestion

Newly synthesized proteins from concentrated media (Amicon Ultra® Centrifugal Filters, 3-kDa cutoff, Millipore) (250 µl) were enriched using the Click-iT® Protein Enrichment Kit (Invitrogen), applying the vendor's protocol with slight modifications, as described previously (12). One-hundred microliters of agarose resin slurry was used, and the volumes of all reagents were divided by two. After washing the resin with 900 µL water, the concentrated media, diluted in 250 µL urea buffer, and catalyst solution were added and incubated for 16-20 h at room temperature. After washing the resin with 900 µL water, 0.5 mL SDS buffer and 0.5 µL 1 M dithiothreitol (DTT) (Bio-Rad) were added and vortexed at 70°C for 15 min. The supernatant was aspirated, and 3.7 mg iodoacetamide (Bio-Rad) was added and incubated for 30 min in the dark.

The resin was transferred to a spin column (supplied with the kit) and washed with 20 mL of SDS buffer, 20 mL of 8 M urea in 100 mM Tris, pH 8, 20 mL of 20% isopropanol and 20 mL of 20% acetonitrile. After dissolving the resin in digestion buffer (100 mM Tris, pH 8, 2 mM $CaCl_2$ and 10% acetonitrile), 0.5 µg trypsin (Promega) was added and incubated overnight at 37°C. The peptide solution was collected, and the resin was washed with 500 µL water. Both solutions were combined and acidified with 20 µL 10% CF_3COOH.

Sample Preparation for Mass Spectrometry

The acidified samples were desalted using Sep-Pak® cartridges (Vac 1 cc (50 mg) tC18, Waters) and fractionated (into 12 fractions) using isoelectric focusing on an Agilent 3100 OFFGEL Fractionator in combination with Immobiline® DryStrips (ph 3–10 NL, 13 cm, GE Healthcare). Focusing was performed at a constant current of 50 mA with a maximum voltage of 4000 V. After reaching 20 kVh, the samples were collected, acidified with CF_3COOH, and desalted using StageTips (13). The peptide samples were dried and dissolved in 4% acetonitrile, 0.1% formic acid.

LC-MS/MS

Peptides were separated using a nanoAcquity ultra performance liquid chromatography (UPLC) system (Waters) fitted with a trapping (nanoAcquity Symmetry C_{18}, 5 µm, 180 µm × 20 mm) and an analytical column (nanoAcquity BEH C_{18}, 1.7 µm, 75 µm × 200 mm). The outlet of the analytical column was coupled directly to an Orbitrap Velos Pro (Thermo Fisher Scientific) using a Proxeon nanospray source (solvent A, 0.1% formic acid; solvent B, acetonitrile and 0.1% formic acid). The samples were loaded with a constant flow of solvent A at 15 µL per min onto the trapping column. Peptides were eluted through the analytical column at a constant flow of 0.3 µL per min. During the elution step, the percentage of solvent B increased in a linear fashion from 3% to 25% in 110 min, which was followed by an increase to 40% in 10 min and an increase to 85% in 1 min. The peptides were introduced into the mass spectrometer by a Pico-Tip Emitter 360 µm OD × 20 µm ID; 10

µm tip (New Objective). Full scan mass spectrometry spectra with mass range 300–1,700 mass-to-charge ratio (m/z) were acquired in profile mode in the orbitrap with a resolution of 30,000. The filling time was set at maximum of 500 ms with a limitation of 10^6 ions. The most intense ions (up to 15) from the full-scan mass spectrometry were selected for fragmentation in the LTQ. A normalized collision energy of 40% was used, and the fragmentation was performed after accumulation of 3×10^4 ions or after a filling time of 100 ms for each precursor ion (whichever occurred first). MS/MS data were acquired in centroid mode. Only multiply charged (2+ or 3+) precursor ions were selected for MS/MS. The dynamic exclusion list was restricted to 500 entries, with a maximum retention period of 30 s and a relative mass window of 10 ppm. Lock mass correction using a background ion (m/z 445.12003) was applied.

Data processing

The mass spectrometric raw data were processed using MaxQuant (version 1.3.0.5) (14) and MS/MS spectra were searched using the Andromeda search engine (15) against mouse (75,721 entries, downloaded 20.02.2013) proteins in UniProt, concatenated to the bovine-specific portion of UniProt (26,526 entries, downloaded 21.06. 2011), to which 247 frequently observed contaminants and reversed sequences of all entries had been added. Enzyme specificity was set to trypsin/P, and a maximum of two missed cleavages were allowed. Cysteine carbamidomethylation was used as the fixed modification and methionine oxidation, protein N-terminal acetylation and replacement of methionine by AHA were used as variable modifications. The minimal peptide length was set to 6 amino acids. The initial maximal allowed mass tolerance was set to 20 ppm for peptide masses and then was set to 6 ppm in the main search and to 0.5 Da for fragment ion masses. FDRs for peptide and protein identification were set to 1%. At least one unique peptide was required for protein identification. The protein identification was reported as an indistinguishable 'protein group' if no unique peptide sequence to a single database entry was identified.

For protein quantification, a minimum of two ratio counts was set and the 'requantify' and 'match between runs' functions were enabled. A protein group was kept for further analysis if it contained at least one mouse sequence and the number of identified peptide species carrying an intermediate or heavy label divided by the total number of peptide species detected in the complete experimental setup was higher than 0.2. Data are available via ProteomeXchange (16) with the identifier PXD009280.

Statistical analysis

Only proteins that have been quantified in at least two of the three replicates have been used for statistical analysis. In a first standardization step, the $\log_2$ distributions of available protein ratios per replicate sample

have been centered around zero. Then a linear model had been fitted to those centered data, which was subjected to an empirical Bayes moderated t-test using the Limma package (version 3.30.13) in R/Bioconductor (version 3.3.2) (17). In order to fully embrace the potential of the presented datasets and to give a complete picture of differential secretion we report the default output of adjusted p-values implemented in LIMMA. This p-value adjustment controls false discovery rates and is based on Benjamini and Hochberg's method. Proteins with an adjusted p-value of less than 0.05 were considered to be differentially secreted and those results should be interpreted in a way that within the group of differentially secreted proteins a fraction of 5% is expected to be false discoveries. Data visualization was performed with the ggplot2 package (version 2.2.1) and included annotations derived from Gene Ontology (GO).

Gene Ontology enrichment analysis

The enrichment analysis for Gene Ontology (GO) annotation terms was performed using DAVID Bionformatics Resources 6.8 (https://david.ncifcrf.gov/home.jsp) (18). The background set was all the differentially secreted proteins in the particular secretome analysis. The p-value cut-off for the GO enrichment was 0.1 (EASE 0.1).

Results

White adipocytes secrete more proteins involved in carbohydrate metabolism while brown adipocytes secrete more extracellular matrix proteins

We were interested how the secretome of primary murine white and brown adipocytes changes upon stimulation with norepinephrine (NE). We investigated this by performing comparative secretome studies using a combination of AHA and pSILAC labeling (Figure 1) (Eichelbaum, Winter et al., 2012). In total, we identified 1,337 unique proteins in three different analyses that showed detectable signals in at least one condition (Supplemental table 1A) and 499 unique proteins that showed detectable signals in at least two (Supplemental table 1B). For all subsequent analyses, the latter list of 499 proteins was used.

In the first analysis, we compared the secretome of white and brown adipocytes at basal conditions (i.e. without NE stimulation) and obtained 141 significantly differentially secreted proteins (p-adj < 0.05, nominal p-value cutoff = 0.023, Figure 2A, Supplemental table 2). As adipocytes secrete a number of known secreted factors called adipokines, we first investigated whether we can identify known adipokines as positive controls. Indeed, we were able to identify well-known classical adipokines like adipsin (complement factor D, CFD), adiponectin (ADIPOQ) and resistin (RETN). In addition, we also found lesser-known adipokines like sparc-like

1 (SPARCL1), spondin-1 (SPON1), dermatopontin (DPT), C-C motif chemokine 8 (CCL8) and matrix metalloproteinase-14 (MMP14) (Figure 2A), thus supporting the validity of our approach. SPON1 showed a 5-fold increased secretion in white adipocytes and was the highest differentially secreted protein from white adipocytes. It was first identified as adipokine secreted from white adipocytes in rats and its secretion was shown to be regulated by insulin resistance (19). In addition, it has been suggested to promote growth and guidance of the axons (20). All these adipokines exhibited a more pronounced secretion in white adipocytes, but interestingly, they were also secreted from brown adipocytes. Moreover, we also found two other adipokines, collagen alpha-2(I) chain and collagen alpha-2(V) chain, known to be secreted from 3T3-L1 white adipocytes during adipogenesis, to be 4-fold and 2-fold higher secreted from brown compared to white adipocytes, respectively. Thus, this analysis demonstrated that a number of well-known white adipocyte-derived adipokines are also, if not even higher, secreted from brown adipocytes.

Next, we were interested in associating unique biological processes to the secreted proteins. Thus, we applied GO term enrichment analysis to the significantly differentially secreted proteins. This enrichment analysis yielded '*Carbohydrate metabolic process*' as the most enriched GO term for the proteins with increased secretion from white adipocytes (Figure 2B upper panel, Supplemental table 3) confirming one of their main functions being the storage of excess carbohydrates in the form of triglycerides. Proteins enriched in this term include glyceraldehyde-3-phosphate dehydrogenase (GAPDH) and insulin growth factor 2 (IGF2) (Figure 2C). 'Oxidation-reduction' process was the second GO term enriched and included the proteins catalase (CAT) and fatty acid synthase (FASN). Catalase, a potent anti-oxidant enzyme, correlates in expression levels with adipogenesis in a PPARγ-dependent manner (21) while the secretion of fatty acid synthase, a key enzyme in de novo lipogenesis, is increased during nutrient deprivation by AMPK activation (22). Interestingly, no GO term was significantly enriched for proteins preferentially secreted from brown adipocytes indicating a broader range of secreted protein classes.

The majority of identified factors were not known to be secreted by either white or brown adipocytes, thus they have not been recognized as potential adipokines before. The two most highly secreted proteins from the brown adipocytes were Lysozyme C-2 (LYZ2) and cathepsin S (CTSS) (Figure 2C). These catalytic enzymes are both components of the extracellular matrix (ECM), with CTSS exhibiting pro-inflammatory properties (23). Interestingly, other highly secreted proteins from brown adipocytes were collagen α1 and α2 chains belonging to type I, III, and IV collagen fibers (Figure 2C). This indicates that brown adipocytes preferentially secrete higher amounts of ECM proteins compared to white adipocytes.

Norepinephrine triggers an increased secretion of classical known adipokines in white adipocytes and of novel adipokines in brown adipocytes

The sympathetic nervous system tightly regulates the function of WAT and BAT via norepinephrine (NE). This neurotransmitter is a potent stimulant for adipocytes: it primarily activates lipolysis in white adipocytes, thermogenesis in brown adipocytes as well as brown-like characteristics during adipogenesis. However, as the NE-induced secretory response of adipocytes has not been established yet, we investigated how the NE-induced secretome differs between white and brown adipocytes. We treated SVF-derived differentiated primary white and brown adipocytes with NE for 24 hours and obtained 186 significantly differentially secreted proteins (p-adj < 0.05, nominal p-value cutoff = 0.024, Figure 3A, Supplemental table 5). Among this large number of secreted proteins, we detected the afore-mentioned adipokines similar to the first analysis (Figure 3A). In addition, we found three proteins to be responsive to NE, known to be secreted from white adipocytes, i.e. osteopontin (SPP1) that promotes inflammation and macrophage infiltration in adipose tissue, lipoprotein lipase (LPL) that hydrolyzes triglycerides from chylomicrons and very low density lipoproteins (VLDLs) and ectonucleotide pyrophosphatase/ phosphodiesterase family member 2 (ENPP2) that catalyzes the formation of lysophosphatidic acid (LPA) in extracellular fluids (24-26) (Figure 3A). However, in addition to these known adipokines, there were several adipokine candidates not known so far to be secreted by white or brown adipocytes upon NE treatment.

GO enrichment analysis revealed that the overall profile of the NE-induced secretome of white and brown adipocytes was very different (Figure 3B, Supplemental table 6 and 7). Surprisingly, the GO term '*Tricarboxylic acid*' was enriched among the proteins that were more secreted from white than from brown adipocytes. This term included proteins like isocitrate dehydrogenase 1 (IDH1) and aconitase 2 (ACO2), indicating a possible novel function outside their primary location in the cytosol or mitochondria. Similar to the previous analysis (Figure 2B lower panel) and despite the large number of significantly differentially secreted proteins no GO term for biological processes was enriched among the proteins favoring higher secretion from brown adipocytes, again indicating a broad secretory response from brown adipocytes.

In response to NE, the most differentially secreted protein from white compared to brown adipocytes was major urinary protein 2 (MUP2) with a 5.6-fold change. Major urinary protein 2 is a novel adipokine candidate, belonging to the family of major urinary proteins that are known to regulate glucose and lipid metabolism and increase energy expenditure (27, 28) (Figure 3C). Spondin-1 and resistin were the second and third most differentially secreted proteins with 5-fold and 4-fold higher secretion from white compared to brown

adipocytes, respectively. Other well-known adipokines like adipsin and adiponectin were also among the highest differentially secreted proteins (Figure 3C). Thus, the majority of the proteins with highest secretion in white compared to brown adipocytes upon NE treatment were well-known adipokines.

In response to NE in brown adipocytes, we identified lysozyme C-2, collagen alpha-1(VIII) chain (COL8A1), chemokine (C-C motif) ligand 9 (CCL9), cathepsin S and collagen alpha-2(I) chain as novel and top highest secreted proteins compared to white adipocytes (Figure 3C). Thus, lysozyme C-2, cathepsin S and collagen alpha-2(I) chain were higher secreted from brown adipocytes, with and without NE stimulation. Chemokine (C-C motif) ligand 9 is a unique member of the CC chemokine family that promotes preadipocyte recruitment and modulates adipogenesis in white adipocytes (29). However, the physiological implications of its 4-fold higher secretion upon NE treatment from brown adipocytes compared to white adipocytes needs further investigation. Collagen alpha-1(VIII) chain (COL8A1), including the vastatin fragment, was also secreted 4-fold higher from NE treated brown adipocytes than white adipocytes (Figure 3C). We speculate that the increased secretion of collagen alpha-1(VIII) chain upon NE treatment in brown adipocytes promotes proliferation and adipogenesis via PI3K/AKT signaling (30, 31). Other novel adipokines that showed increased 3-fold secretion in this condition were heme oxygenase 1 and beta-nerve growth factor (Supplemental table 5). We summarize that in white adipocytes, the top secreted proteins upon NE stimulation are well-known classical adipokines, while in brown adipocytes, novel adipokine candidates are the top secreted proteins.

The secretory response between NE-stimulated and basal state is complex involving lipolysis, glucose uptake, browning of white adipocytes and protection against oxidative damage

In addition to the comparative secretome analyses between white and brown adipocytes (i.e. Figure 2A and 3A), we were also interested in proteins whose secretion was significantly altered upon NE treatment in comparison to the unstimulated state. For this purpose, we analyzed the combined data of the significantly differentially secreted proteins from the two analyses above (Figure 4). The combination of two independent variables, the type of adipocyte and stimulation with NE, led to the division of the scatterplot into four quadrants: Q1 – Q4. Proteins, which do not change in secretion upon NE treatment compared to the unstimulated state, or change in secretion to a similar degree between white and brown adipocytes, are along the diagonal.

In Q1, the afore-mentioned adipokines adipsin (CFD) and catalase (CAT) increased most in their secretion from white adipocytes upon NE treatment with a 2.6-fold and 2.8-fold increase from basal state, respectively (Figure 4). In addition, most of the known adipokines mentioned earlier like ectonucleotide pyrophosphatase/

phosphodiesterase family member 2, lipoprotein lipase, adiponectin and resistin were increased in secretion from white adipocytes upon NE treatment.

Oppositely, in Q3, NE stimulation increased the secretion of collagen alpha-1(VIII) chain (COL8A1), galectin-3 (LGALS3) and osteopontin (SPP1) in brown adipocytes (Figure 4). Glucose uptake via Glut4 is important for brown adipocytes, and galectin-3 was found to be crucial for Glut4-mediated glucose utilization in skeletal muscle and aortic endothelium (32). Galectin-3 has also been shown to promote adipogenesis (33). Thus, NE-stimulated elevation of galectin-3 secretion from brown adipocytes could modulate adipogenesis and glucose uptake.

Furthermore, in Q2, UDP-glucose 6-dehydrogenase (UGDH) showed a 3-fold increase in secretion from white to brown adipocytes upon NE treatment. UDP-glucose 6-dehydrogenase is an extracellular matrix enzyme responsible for the synthesis of hyaluronan (HA) and is important for tissue organization, development and cell proliferation (34). Given that hyaluronan is a major component of the adipose tissue ECM and affects adipogenesis and adipose tissue function (35), we speculate that UDP-glucose 6-dehydrogenase mediates these effects via hyaluronan in NE-treated brown adipocytes. On the other hand, insulin growth factor 2 (IGF2), a fetal mitogen, showed a 5-fold higher secretion in white adipocytes in the basal state (Figure 2A) but this differential secretion was abolished with NE treatment. We cannot conclude whether IGF2 secretion from brown adipocytes increased or white adipocyte secretion decreased with NE treatment resulting in no differential secretion. As IGF2 causes a decrease in white and brown adipogenesis, we speculate that the latter scenario occurs in order to abolish this inhibitory effect on adipogenesis upon NE treatment (36, 37).

Interestingly, in Q4, collagen type V alpha 3 chain (COL5A3) showed a secretion with 2-fold differential increase in white adipocytes. This collagen V chain is highly expressed in white adipocytes and is an important ECM component responsible for glucose homeostasis and adipose tissue expansion (38). Compared to Q2, only a few proteins in Q4 strongly changed their secretion ratios, thus we identified more relative changes in secretion favoring brown adipocytes upon NE stimulation.

In summary, by comparing the secretome of white and brown adipocytes in their basal and NE-stimulated state, we identified a number of secreted proteins responsive to NE treatment. These proteins are involved in various adipocyte processes like ECM organization, lipolysis, adipogenesis, glucose uptake, and protection against oxidative damage.

Norepinephrine stimulation of primary brown adipocytes broadly and significantly changes the secretion of batokines

The previously described analyses gave us an insight into the secretome differences between white and brown adipocytes, in the presence or absence of NE, but they do not reveal NE-induced changes in the brown adipocyte secretome itself. Therefore, we treated SVF-derived, differentiated brown adipocytes with NE for 24 hours and compared their secretome to that of untreated brown adipocytes and obtained 280 significantly differentially secreted proteins (p-adj < 0.05, nominal p-value cutoff = 0.039, Figure 5A, Supplemental table 8). Among these 280 proteins, the afore-mentioned known adipokines lipoprotein lipase, adipsin, ectonucleotide pyrophosphatase/phosphodiesterase family member 2, adiponectin, collagen alpha-2(I) chain, collagen alpha-2(V) chain, SPARC-like protein 1, dermatopontin and osteopontin showed enhanced secretion from brown adipocytes without NE stimulation (Figure 5A). Moreover, we found that angiopoietin-like 4 (ANGPTL4), an adipokine highly expressed in brown adipocytes (39), is also secreted. Interestingly, the secretion of ANGPTL4 was repressed by NE treatment, which coincides with its decreased expression in brown adipocytes upon cold exposure (40).

GO enrichment analysis revealed '*Protein folding'* as the most significantly enriched term for the NE-induced proteins (Figure 5B, Supplemental table 9). This GO term included heat shock protein 8 (HSPA8) and peptidylprolyl isomerase A (PPIA) which are integral components of chaperone-mediated autophagy (CMA) preceding lipolysis (41) and adipogenesis (42), respectively (Figure 5C). '*Oxidation-reduction process*' was the second most significantly enriched term upon NE treatment. Proteins belonging to this GO term comprised catalase, heme oxygenase 1, thioredoxin 1, and members of the peroxiredoxin family. These proteins and enzymes exhibit strong anti-oxidative properties, which could protect brown adipocytes against NE-triggered rise in reactive oxygen species (ROS) production (43).

On the other hand, proteins with higher secretion without NE stimulation were enriched for GO terms associated with ECM organization and angiogenesis (Figure 5B lower panel, Supplemental table 10). Some of these include galectin-3 ('*Cell adhesion*'), SPARC-related modular calcium-binding protein 1 ('*Extracellular matrix organization*') and plasminogen activator ('*Angiogenesis*'). Thus, in brown adipocytes NE-induced secreted proteins were involved in several important metabolic and oxidation-reduction processes, in particular anti-oxidative proteins, while the secretion of proteins associated with ECM organization and angiogenesis decreased (Figure 5C). Interestingly, while we found ECM proteins to be higher secreted in brown than white adipocytes in the unstimulated state (chapter 1), the secretion of ECM proteins was diminished by NE.

Among the NE-induced proteins, fatty acid binding protein 4 (FABP4), a lipid transport protein crucial for BAT thermogenesis, exhibited the highest (10.5-fold) increase in secretion followed by galectin-3 (8.5-fold) (Figure 5C). Studies have shown that FABP4 is required for uptake of non-esterified fatty acids and storage of triglycerides in BAT. Accordingly, FABP4 and FABP5 double knockout mice exhibit impaired thermogenesis due to depletion of BAT energy stores (44). Interestingly, the secretion of FABP5 was also increased 4-fold upon NE treatment in our analysis.

Among the NE-repressed proteins, we identified apoliprotein E (APOE) and lipoprotein lipase, both involved in the uptake and lipolysis of chylomicrons and VLDLs, as proteins with the strongest decrease (20-fold and 12-fold, respectively) in secretion (Figure 5C). However, the resultant physiological consequence of this reduced secretion is unclear since BAT mainly replenishes its intracellular triglyceride stocks via lipolysis mediated uptake of lipoprotein-derived fatty acids (45, 46). Interestingly, we also found galectin-3 binding protein (LGALS3BP), a binding partner of galectin-3 (GAL-3), to be significantly reduced in secretion upon NE treatment, as opposed to GAL-3 whose secretion increased. LGALS3BP and GAL-3 are under different transcriptional regulation and together mediate cell-cell adhesion (47). A recent study described a secondary function of LGALS3BP in affecting Wnt signaling by binding Wnt ligands and improving their storage, spread and bioavailability (48). As Wnt proteins block brown adipogenesis, it may be speculated that NE contributes to reduced secretion of LGALS3BP to indirectly reduce intracellular Wnt signaling in brown adipocytes (49).

Discussion

There are a number of studies on the secretome of white adipocytes, in mice and humans (50-53). However, a comparative proteomic analysis of secreted factors from white and brown adipocytes has not been reported yet, despite the fact that BAT, like its white counterpart, also exhibits an endocrine function by secreting adipokines, called batokines or brown adipokines. Herein, we have studied the secretome of murine SVF-derived primary white and brown adipocytes by using mass spectrometry combined with AHA labelling and pulsed SILAC with the aim of characterizing the white and brown adipocyte secretome and identifying potential novel adipokine candidates. We had developed this approach to analyze the secretome of primary hepatocytes and Hepa 1-6 cells, LPS-stimulated macrophages, and PC3 and WPMY-1 cells under serum starvation (12). The use of click-chemistry offers two main advantages in the study of the adipocyte secretome. Firstly, the primary adipocytes could be cultured in media containing serum, which prevents changes in growth conditions and in the native secretome. Most secretome approaches have to avoid the use

of serum to reduce contamination and facilitate detection of genuine secretory proteins. With our methodology, the substitution of methionine with AHA in the cellular proteome enables the selective enrichment of secreted proteins from the supernatant thereby reducing contamination by serum proteins. Secondly, AHA labelling circumvents extensive time-consuming peptide fractionation owing to the selective enrichment and thus reduced sample complexity, which expedites the whole secretome analysis. The reliability of this technique was evident in the high correlation between the replicates in each analysis (Figure S1) and the detection of several well-known adipokines.

A confounding factor in classical secretome analysis is the inability to distinguish genuine secretory proteins from those that originate from lysed cells. An added advantage of our methodology is that it is far less sensitive to this phenomenon. Specifically, our approach relies on the detection of newly synthesized proteins that have incorporated AHA and SILAC amino acids during the experiment. By definition, this can only occur in intact living cells. If broken cells are present at all (which cannot be excluded), their (unlabeled) proteins will be removed during the AHA-enrichment, along with serum proteins that are present in high abundance but that similarly lack AHA. In the worst case, if cells break during cell incubation, it is reasonable to expect that this occurs to the same degree between compared conditions (e.g. +/- NE). Such cases would be disregarded in our data since we were primarily interested in proteins that are differentially secreted, i.e. that derive from secretory activity and not from cell damage. In line with this, we could not observe any prominent visual indicators of cell death during the incubation of adipocytes with AHA-supplemented SILAC media. To obtain a quantitative estimate, we measured the percentage of cell death by measuring LDH release in AHA-supplemented growth media in a pilot study and found that there is about 20% cell death among the adipocytes with no increase after 24 hours (Figure S2A). As this is the same media used in the secretome analysis, it can be concluded that after the first 24 hours there is no significant rise in cell death.

Other studies have focused on the white adipocyte secretome in various settings like adipogenesis (54), insulin resistance (55) and depot-specific differences (56). However, no one so far has investigated the secretome response induced by norepinephrine (NE), a catecholamine that mediates essential physiological responses. Here we provide the first systematic study investigating the brown adipocyte secretome – in addition to the white adipocyte secretome – and their response to NE. We accomplished this by conducting three comparative analyses: the first two compared the secretome of white and brown adipocytes without and with NE treatment, respectively (Figure 2 and 3), while the third experiment compared brown adipocytes with and without NE stimulation (Figure 5). Our study revealed that i) in the absence of NE carbohydrate

metabolism-regulating proteins are favored in the white adipocyte secretome, while no specific protein class is predominant in the brown adipocyte secretome (Figure 2B), ii) in white adipocytes NE triggers increased secretion of several well-known adipokines, while it promotes secretion of novel adipokines in brown adipocytes (Figure 3C), iii) the secretory response between NE-stimulated and basal state is diverse ranging from glucose and lipid metabolism to adipogenesis and resistance to oxidative stress (Figure 4), and iv) the brown adipocyte secretome is substantially altered upon NE treatment (Figure 5C).

As expected, proteins involved in carbohydrate metabolism were enriched in white adipocytes without NE treatment when compared to brown adipocytes (Figure 2B). However, finding an enrichment for tricarboxylic acid proteins in white adipocytes upon treatment with NE was unexpected as the TCA takes place in the inner mitochondrial membrane and most of the proteins were annotated as mitochondrial proteins. The analysis in brown adipocytes with and without NE revealed that the majority of brown adipokines with NE-increased secretion are involved in redox reactions like peroxiredoxin-4, catalase and heme oxygenase 1 (Figure 5B). An often made association with ROS production and oxidative stress in brown adipocytes has been UCP1 activation and mitochondrial uncoupling. While Shabalina and colleagues have shown that UCP1 is not involved in control of ROS production in brown-fat mitochondria (57), several studies have shown that UCP1 plays an important and evolutionary conserved function in the reduction of superoxide production (58-60). Stier and colleagues also demonstrated that cold-exposure activated UCP1 in BAT allowed wildtype mice to increase their metabolism to generate heat while preventing damage by oxidative stress (61). Interestingly, we observed a distinct secretory profile between white and brown adipocytes, and our findings suggest that brown adipocyte secreted factors may indeed contribute to prevent NE-induced oxidative stress along with activated UCP1. Moreover, in our comparison of the white and brown adipocyte secretome in the NE-stimulated and unstimulated state, we observed that NE increased the differential secretion of most classical adipokines like adiponectin, adipsin and resistin in white adipocytes while novel adipokines like osteopontin and galectin-3 were more highly secreted in brown adipocytes (Figure 4). This observation underscores our findings that i) most well-known adipokines are in fact NE-responsive white adipocyte-enriched secreted proteins and ii) the majority of the NE-responsive brown adipocyte-enriched secreted proteins are novel uncharacterized adipokines, a treasure trove of metabolic regulators that await further functional characterization.

As outlined above, we detected several well-known adipokines like adipsin, adiponectin and resistin in our analyses (Suppl. Table 2), but not others such as tumor necrosis factor α, interleukin-6 and leptin, similar to

Adachi, Kumar et al. (62). However, their lack of detection does not necessarily mean their lack of secretion. This is especially true for leptin that was absent in several other secretome screens (63) and was only detectable using antibody-based methods (64, 65) leading to the speculation that leptin's structural properties reduce its detectability by mass spectrometric analysis. Indeed, we were also able to detect leptin (and resistin) using the MILLIPLEX® MAP Mouse Metabolic Hormone panel on the Luminex xMAP® platform (MAGPIX®) from both white and brown adipocytes after 6 and 24 hours of incubation with fresh growth media (Figure S2B). The detection of resistin secretion in white and brown adipocytes by this method nicely recapitulated the secretion ratio determined in our secretome analysis.

Moreover, even for the well-known classical adipokines like adiponectin and resistin, we uncovered valuable novel insight into their secretion profile from white and brown adipocytes. The secretion of adiponectin was not drastically different in the basal state among white and brown adipocytes (Figure 2), but was higher upon NE from white compared to brown adipocytes (Figure 3), partly because of reduced secretion from brown adipocytes by 7-fold upon NE treatment (Figure 5). As adiponectin suppresses thermogenesis by inhibiting UCP1 expression, its decreased secretion in brown adipocytes could prevent the autocrine inhibition of thermogenesis (66). For resistin the secreted levels were higher from white than brown adipocytes and this difference was further increased upon NE stimulation. Similar to adiponectin, NE-mediated decrease in secretion of resistin from brown adipocytes diminishes its negative autocrine effects on BAT activity and adipogenesis (67).

In terms of novel batokine candidates, galectin-3 and osteopontin are two interesting proteins that were detected in our study. Galectin-3 is a member of the lectin family known to be protective in obesity (68) and inflammation (69). In our analyses, its secretion was not different in the absence of NE but was 2.5-fold higher upon NE stimulation in brown compared to white adipocytes (explained by an 8-fold increase upon NE treatment in brown adipocytes). The afore-mentioned decrease in adiponectin secretion fits with the increase in galectin-3 secretion as adiponectin represses the secretion of galectin-3 from adipocytes (70). These observations point to an important role of galectin-3 in propagating beneficial effects of NE-stimulated BAT activity possibly by regulating inflammation and/or promoting thermogenesis. In addition, we found osteopontin secretion to be responsive to NE treatment, with a 4-fold increase in brown adipocytes (Figure 5) leading to 2-fold stronger increase in brown compared to white adipocytes (Figure 3). Osteopontin is an extracellular matrix protein involved in biomineralization, tissue remodeling and inflammation (71). It is primarily associated with bone metabolism and remodeling, but has also been associated with obesity and

insulin resistance (72, 73) and is a putative link between bone homeostasis and adipose tissue (74). We speculate that osteopontin released by activated BAT may be responsible for the positive correlation observed between bone anabolism/remodeling and BAT volume (75).

In summary, we obtained novel secretion profiles of known adipokines and novel adipokine candidates from brown and white adipocytes, and provide a large resource of significantly differentially secreted proteins: 141 between white and brown adipocytes (Figure 2), 186 between white and brown adipocytes upon NE treatment (Figure 3) and 280 responsive to NE from brown adipocytes, with most of them being novel adipokines (Figure 5). Furthermore, we not only present novel secretory profiles for individual proteins but also functionally enriched protein classes which were significantly changed between white and brown adipocytes and were responsive to NE stimulation. To conclude, with our study, we provide a comprehensive catalogue of novel adipokine candidates secreted from white and brown adipocytes and responsive to NE, which may serve as basis for numerous hypothesis-driven functional studies in the near future for characterizing adipocyte-secreted proteins. Given the beneficial effects of BAT activation on systemic metabolism and its endocrine function, this study provides an archive of potential brown adipokines and biomarkers for activated BAT.

References

1. Rosen, E. D., and Spiegelman, B. M. (2006) Adipocytes as regulators of energy balance and glucose homeostasis. *Nature* 444, 847-853

2. Arita, Y., Kihara, S., Ouchi, N., Takahashi, M., Maeda, K., Miyagawa, J., Hotta, K., Shimomura, I., Nakamura, T., Miyaoka, K., Kuriyama, H., Nishida, M., Yamashita, S., Okubo, K., Matsubara, K., Muraguchi, M., Ohmoto, Y., Funahashi, T., and Matsuzawa, Y. (1999) Paradoxical decrease of an adipose-specific protein, adiponectin, in obesity. *Biochem Biophys Res Commun* 257, 79-83

3. Bukowiecki, L. J. (1989) Energy balance and diabetes. The effects of cold exposure, exercise training, and diet composition on glucose tolerance and glucose metabolism in rat peripheral tissues. *Can J Physiol Pharmacol* 67, 382-393

4. Cypess, A. M., Lehman, S., Williams, G., Tal, I., Rodman, D., Goldfine, A. B., Kuo, F. C., Palmer, E. L., Tseng, Y., Doria, A., Kolodny, G. M., and Kahn, C. R. (2009) Identification and Importance of Brown Adipose Tissue in Adult Humans. *New England Journal of Medicine* 360, 1509-1517

5. Yamauchi, T., Kamon, J., Waki, H., Terauchi, Y., Kubota, N., Hara, K., Mori, Y., Ide, T., Murakami, K., Tsuboyama-Kasaoka, N., Ezaki, O., Akanuma, Y., Gavrilova, O., Vinson, C., Reitman, M. L., Kagechika, H., Shudo, K., Yoda, M., Nakano, Y., Tobe, K., Nagai, R., Kimura, S., Tomita, M., Froguel, P., and Kadowaki, T. (2001) The fat-derived hormone adiponectin reverses insulin resistance associated with both lipoatrophy and obesity. *Nature Medicine* 7, 941-946

6. Lazar, M. A. (2007) Resistin- and Obesity-associated metabolic diseases. *Horm Metab Res* 39, 710-716

7. Fruhbeck, G. (2002) Peripheral actions of leptin and its involvement in disease. *Nutr Rev* 60, S47-55; discussion S68-84, 85-47

8. Villarroya, F., Cereijo, R., Villarroya, J., and Giralt, M. (2017) Brown adipose tissue as a secretory organ. *Nat Rev Endocrinol* 13, 26-35

9. Enerback, S., Jacobsson, A., Simpson, E. M., Guerra, C., Yamashita, H., Harper, M. E., and Kozak, L. P. (1997) Mice lacking mitochondrial uncoupling protein are cold-sensitive but not obese. *Nature* 387, 90-94

10. Lowell, B. B., V, S. S., Hamann, A., Lawitts, J. A., Himms-Hagen, J., Boyer, B. B., Kozak, L. P., and Flier, J. S. (1993) Development of obesity in transgenic mice after genetic ablation of brown adipose tissue. *Nature* 366, 740-742

11. Villarroya, F., Gavalda-Navarro, A., Peyrou, M., Villarroya, J., and Giralt, M. (2017) The Lives and Times of Brown Adipokines. *Trends Endocrinol Metab* 28, 855-867

12. Eichelbaum, K., Winter, M., Berriel Diaz, M., Herzig, S., and Krijgsveld, J. (2012) Selective enrichment of newly synthesized proteins for quantitative secretome analysis. *Nat Biotechnol* 30, 984-990

13. Rappsilber, J., Ishihama, Y., and Mann, M. (2003) Stop and go extraction tips for matrix-assisted laser desorption/ionization, nanoelectrospray, and LC/MS sample pretreatment in proteomics. *Anal Chem* 75, 663-670

14. Cox, J., and Mann, M. (2008) MaxQuant enables high peptide identification rates, individualized p.p.b.-range mass accuracies and proteome-wide protein quantification. *Nat Biotechnol* 26, 1367-1372

15. Cox, J., Neuhauser, N., Michalski, A., Scheltema, R. A., Olsen, J. V., and Mann, M. (2011) Andromeda: a peptide search engine integrated into the MaxQuant environment. *J Proteome Res* 10, 1794-1805

16. Vizcaino, J. A., Cote, R. G., Csordas, A., Dianes, J. A., Fabregat, A., Foster, J. M., Griss, J., Alpi, E., Birim, M., Contell, J., O'Kelly, G., Schoenegger, A., Ovelleiro, D., Perez-Riverol, Y., Reisinger, F., Rios, D., Wang, R., and Hermjakob, H. (2013) The PRoteomics IDEntifications (PRIDE) database and associated tools: status in 2013. *Nucleic Acids Res* 41, D1063-1069

17. Gentleman, R. C., Carey, V. J., Bates, D. M., Bolstad, B., Dettling, M., Dudoit, S., Ellis, B., Gautier, L., Ge, Y., Gentry, J., Hornik, K., Hothorn, T., Huber, W., Iacus, S., Irizarry, R., Leisch, F., Li, C., Maechler, M., Rossini, A. J., Sawitzki, G., Smith, C., Smyth, G., Tierney, L., Yang, J. Y., and Zhang, J. (2004) Bioconductor: open software development for computational biology and bioinformatics. *Genome Biol* 5, R80

18. Dennis, G., Jr., Sherman, B. T., Hosack, D. A., Yang, J., Gao, W., Lane, H. C., and Lempicki, R. A. (2003) DAVID: Database for Annotation, Visualization, and Integrated Discovery. *Genome Biol* 4, P3

19. Lim, J. M., Sherling, D., Teo, C. F., Hausman, D. B., Lin, D., and Wells, L. (2008) Defining the regulated secreted proteome of rodent adipocytes upon the induction of insulin resistance. *J Proteome Res* 7, 1251-1263

20. Klar, A., Baldassare, M., and Jessell, T. M. (1992) F-spondin: a gene expressed at high levels in the floor plate encodes a secreted protein that promotes neural cell adhesion and neurite extension. *Cell* 69, 95-110

21. Okuno, Y., Matsuda, M., Kobayashi, H., Morita, K., Suzuki, E., Fukuhara, A., Komuro, R., Shimabukuro, M., and Shimomura, I. (2008) Adipose expression of catalase is regulated via a novel remote PPARgamma-responsive region. *Biochem Biophys Res Commun* 366, 698-704

22. Fernandez-Real, J. M., Menendez, J. A., Moreno-Navarrete, J. M., Bluher, M., Vazquez-Martin, A., Vazquez, M. J., Ortega, F., Dieguez, C., Fruhbeck, G., Ricart, W., and Vidal-Puig, A. (2010) Extracellular fatty acid synthase: a possible surrogate biomarker of insulin resistance. *Diabetes* 59, 1506-1511

23. Wendt, W., Lubbert, H., and Stichel, C. C. (2008) Upregulation of cathepsin S in the aging and pathological nervous system of mice. *Brain Res* 1232, 7-20

24. Nomiyama, T., Perez-Tilve, D., Ogawa, D., Gizard, F., Zhao, Y., Heywood, E. B., Jones, K. L., Kawamori, R., Cassis, L. A., Tschop, M. H., and Bruemmer, D. (2007) Osteopontin mediates obesity-induced adipose tissue macrophage infiltration and insulin resistance in mice. *J Clin Invest* 117, 2877-2888

25. Gin, P., Beigneux, A. P., Davies, B., Young, M. F., Ryan, R. O., Bensadoun, A., Fong, L. G., and Young, S. G. (2007) Normal binding of lipoprotein lipase, chylomicrons, and apo-AV to GPIHBP1 containing a G56R amino acid substitution. *Biochim Biophys Acta* 1771, 1464-1468

26. Nishimura, S., Nagasaki, M., Okudaira, S., Aoki, J., Ohmori, T., Ohkawa, R., Nakamura, K., Igarashi, K., Yamashita, H., Eto, K., Uno, K., Hayashi, N., Kadowaki, T., Komuro, I., Yatomi, Y., and Nagai, R. (2014) ENPP2 contributes to adipose tissue expansion and insulin resistance in diet-induced obesity. *Diabetes* 63, 4154-4164

27. Zhou, Y., Jiang, L., and Rui, L. (2009) Identification of MUP1 as a regulator for glucose and lipid metabolism in mice. *J Biol Chem* 284, 11152-11159

28. Hui, X., Zhu, W., Wang, Y., Lam, K. S., Zhang, J., Wu, D., Kraegen, E. W., Li, Y., and Xu, A. (2009) Major urinary protein-1 increases energy expenditure and improves glucose intolerance through enhancing mitochondrial function in skeletal muscle of diabetic mice. *J Biol Chem* 284, 14050-14057

29. Kim, C. S., Kawada, T., Yoo, H., Kwon, B. S., and Yu, R. (2003) Macrophage inflammatory protein-related protein-2, a novel CC chemokine, can regulate preadipocyte migration and adipocyte differentiation. *FEBS Lett* 548, 125-130

30. Li, X., Wang, Z., Tong, H., Yan, Y., and Li, S. (2018) Effects of COL8A1 on the proliferation of muscle-derived satellite cells. *Cell Biol Int*

31. Xia, X., and Serrero, G. (1999) Inhibition of adipose differentiation by phosphatidylinositol 3-kinase inhibitors. *J Cell Physiol* 178, 9-16

32. Darrow, A. L., and Shohet, R. V. (2015) Galectin-3 deficiency exacerbates hyperglycemia and the endothelial response to diabetes. *Cardiovasc Diabetol* 14, 73

33. Baek, J. H., Kim, S. J., Kang, H. G., Lee, H. W., Kim, J. H., Hwang, K. A., Song, J., and Chun, K. H. (2015) Galectin-3 activates PPARgamma and supports white adipose tissue formation and high-fat diet-induced obesity. *Endocrinology* 156, 147-156

34. Viola, M., Vigetti, D., Genasetti, A., Rizzi, M., Karousou, E., Moretto, P., Clerici, M., Bartolini, B., Pallotti, F., De Luca, G., and Passi, A. (2008) Molecular control of the hyaluronan biosynthesis. *Connect Tissue Res* 49, 111-114

35. Zhu, Y., Kruglikov, I. L., Akgul, Y., and Scherer, P. E. (2018) Hyaluronan in adipogenesis, adipose tissue physiology and systemic metabolism. *Matrix Biol*

36. Kleiman, A., Keats, E. C., Chan, N. G., and Khan, Z. A. (2013) Elevated IGF2 prevents leptin induction and terminal adipocyte differentiation in hemangioma stem cells. *Exp Mol Pathol* 94, 126-136

37. Borensztein, M., Viengchareun, S., Montarras, D., Journot, L., Binart, N., Lombes, M., and Dandolo, L. (2012) Double Myod and Igf2 inactivation promotes brown adipose tissue development by increasing Prdm16 expression. *FASEB J* 26, 4584-4591

38. Huang, G., Ge, G., Wang, D., Gopalakrishnan, B., Butz, D. H., Colman, R. J., Nagy, A., and Greenspan, D. S. (2011) alpha3(V) collagen is critical for glucose homeostasis in mice due to effects in pancreatic islets and peripheral tissues. *J Clin Invest* 121, 769-783

39. Kersten, S., Mandard, S., Tan, N. S., Escher, P., Metzger, D., Chambon, P., Gonzalez, F. J., Desvergne, B., and Wahli, W. (2000) Characterization of the fasting-induced adipose factor FIAF, a novel peroxisome proliferator-activated receptor target gene. *J Biol Chem* 275, 28488-28493

40. Dijk, W., Heine, M., Vergnes, L., Boon, M. R., Schaart, G., Hesselink, M. K., Reue, K., van Marken Lichtenbelt, W. D., Olivecrona, G., Rensen, P. C., Heeren, J., and Kersten, S. (2015) ANGPTL4 mediates shuttling of lipid fuel to brown adipose tissue during sustained cold exposure. *Elife* 4

41. Kaushik, S., and Cuervo, A. M. (2015) Degradation of lipid droplet-associated proteins by chaperone-mediated autophagy facilitates lipolysis. *Nat Cell Biol* 17, 759-770

42. Zhang, L., Li, Z., Zhang, B., He, H., and Bai, Y. (2015) PPIA is a novel adipogenic factor implicated in obesity. *Obesity (Silver Spring)* 23, 2093-2100

43. Chouchani, E. T., Kazak, L., Jedrychowski, M. P., Lu, G. Z., Erickson, B. K., Szpyt, J., Pierce, K. A., Laznik-Bogoslavski, D., Vetrivelan, R., Clish, C. B., Robinson, A. J., Gygi, S. P., and Spiegelman, B. M.

(2016) Mitochondrial ROS regulate thermogenic energy expenditure and sulfenylation of UCP1. *Nature* 532, 112-116

44. Syamsunarno, M. R., Iso, T., Yamaguchi, A., Hanaoka, H., Putri, M., Obokata, M., Sunaga, H., Koitabashi, N., Matsui, H., Maeda, K., Endo, K., Tsushima, Y., Yokoyama, T., and Kurabayashi, M. (2014) Fatty acid binding protein 4 and 5 play a crucial role in thermogenesis under the conditions of fasting and cold stress. *PLoS One* 9, e90825

45. Bartelt, A., Bruns, O. T., Reimer, R., Hohenberg, H., Ittrich, H., Peldschus, K., Kaul, M. G., Tromsdorf, U. I., Weller, H., Waurisch, C., Eychmuller, A., Gordts, P. L., Rinninger, F., Bruegelmann, K., Freund, B., Nielsen, P., Merkel, M., and Heeren, J. (2011) Brown adipose tissue activity controls triglyceride clearance. *Nat Med* 17, 200-205

46. Voshol, P. J., Rensen, P. C., van Dijk, K. W., Romijn, J. A., and Havekes, L. M. (2009) Effect of plasma triglyceride metabolism on lipid storage in adipose tissue: studies using genetically engineered mouse models. *Biochim Biophys Acta* 1791, 479-485

47. Inohara, H., Akahani, S., Koths, K., and Raz, A. (1996) Interactions between galectin-3 and Mac-2-binding protein mediate cell-cell adhesion. *Cancer Res* 56, 4530-4534

48. Pikkarainen, T., Nurmi, T., Sasaki, T., Bergmann, U., and Vainio, S. (2017) Role of the extracellular matrix-located Mac-2 binding protein as an interactor of the Wnt proteins. *Biochem Biophys Res Commun* 491, 953-957

49. Kang, S., Bajnok, L., Longo, K. A., Petersen, R. K., Hansen, J. B., Kristiansen, K., and MacDougald, O. A. (2005) Effects of Wnt signaling on brown adipocyte differentiation and metabolism mediated by PGC-1alpha. *Mol Cell Biol* 25, 1272-1282

50. Meissburger, B., Perdikari, A., Moest, H., Muller, S., Geiger, M., and Wolfrum, C. (2016) Regulation of adipogenesis by paracrine factors from adipose stromal-vascular fraction - a link to fat depot-specific differences. *Biochim Biophys Acta* 1861, 1121-1131

51. Alvarez-Llamas, G., Szalowska, E., de Vries, M. P., Weening, D., Landman, K., Hoek, A., Wolffenbuttel, B. H., Roelofsen, H., and Vonk, R. J. (2007) Characterization of the human visceral adipose tissue secretome. *Mol Cell Proteomics* 6, 589-600

52. Dahlman, I., Elsen, M., Tennagels, N., Korn, M., Brockmann, B., Sell, H., Eckel, J., and Arner, P. (2012) Functional annotation of the human fat cell secretome. *Arch Physiol Biochem* 118, 84-91

53. Knebel, B., Goeddeke, S., Poschmann, G., Markgraf, D. F., Jacob, S., Nitzgen, U., Passlack, W., Preuss, C., Dicken, H. D., Stuhler, K., Hartwig, S., Lehr, S., and Kotzka, J. (2017) Novel Insights into the Adipokinome of Obese and Obese/Diabetic Mouse Models. *Int J Mol Sci* 18

54. Zhong, J., Krawczyk, S. A., Chaerkady, R., Huang, H., Goel, R., Bader, J. S., Wong, G. W., Corkey, B. E., and Pandey, A. (2010) Temporal profiling of the secretome during adipogenesis in humans. *J Proteome Res* 9, 5228-5238

55. Lim, J. M., Wollaston-Hayden, E. E., Teo, C. F., Hausman, D., and Wells, L. (2014) Quantitative secretome and glycome of primary human adipocytes during insulin resistance. *Clin Proteomics* 11, 20

56. Roca-Rivada, A., Alonso, J., Al-Massadi, O., Castelao, C., Peinado, J. R., Seoane, L. M., Casanueva, F. F., and Pardo, M. (2011) Secretome analysis of rat adipose tissues shows location-specific roles for each depot type. *J Proteomics* 74, 1068-1079

57. Shabalina, I. G., Vrbacky, M., Pecinova, A., Kalinovich, A. V., Drahota, Z., Houstek, J., Mracek, T., Cannon, B., and Nedergaard, J. (2014) ROS production in brown adipose tissue mitochondria: the question of UCP1-dependence. *Biochim Biophys Acta* 1837, 2017-2030

58. Oelkrug, R., Kutschke, M., Meyer, C. W., Heldmaier, G., and Jastroch, M. (2010) Uncoupling protein 1 decreases superoxide production in brown adipose tissue mitochondria. *J Biol Chem* 285, 21961-21968

59. Oelkrug, R., Goetze, N., Meyer, C. W., and Jastroch, M. (2014) Antioxidant properties of UCP1 are evolutionarily conserved in mammals and buffer mitochondrial reactive oxygen species. *Free Radic Biol Med* 77, 210-216

60. Dlaskova, A., Clarke, K. J., and Porter, R. K. (2010) The role of UCP 1 in production of reactive oxygen species by mitochondria isolated from brown adipose tissue. *Biochim Biophys Acta* 1797, 1470-1476

61. Stier, A., Bize, P., Habold, C., Bouillaud, F., Massemin, S., and Criscuolo, F. (2014) Mitochondrial uncoupling prevents cold-induced oxidative stress: a case study using UCP1 knockout mice. *J Exp Biol* 217, 624-630

62. Adachi, J., Kumar, C., Zhang, Y., and Mann, M. (2007) In-depth analysis of the adipocyte proteome by mass spectrometry and bioinformatics. *Mol Cell Proteomics* 6, 1257-1273

63. Zvonic, S., Lefevre, M., Kilroy, G., Floyd, Z. E., DeLany, J. P., Kheterpal, I., Gravois, A., Dow, R., White, A., Wu, X., and Gimble, J. M. (2007) Secretome of primary cultures of human adipose-derived stem cells: modulation of serpins by adipogenesis. *Mol Cell Proteomics* 6, 18-28

64. Klimcakova, E., Moro, C., Mazzucotelli, A., Lolmede, K., Viguerie, N., Galitzky, J., Stich, V., and Langin, D. (2007) Profiling of adipokines secreted from human subcutaneous adipose tissue in response to PPAR agonists. *Biochem Biophys Res Commun* 358, 897-902

65. Berti, L., Hartwig, S., Irmler, M., Radle, B., Siegel-Axel, D., Beckers, J., Lehr, S., Al-Hasani, H., Haring, H. U., Hrabe de Angelis, M., and Staiger, H. (2016) Impact of fibroblast growth factor 21 on the secretome of human perivascular preadipocytes and adipocytes: a targeted proteomics approach. *Arch Physiol Biochem* 122, 281-288

66. Qiao, L., Yoo, H., Bosco, C., Lee, B., Feng, G. S., Schaack, J., Chi, N. W., and Shao, J. (2014) Adiponectin reduces thermogenesis by inhibiting brown adipose tissue activation in mice. *Diabetologia* 57, 1027-1036

67. Pravenec, M., Mlejnek, P., Zidek, V., Landa, V., Simakova, M., Silhavy, J., Strnad, H., Eigner, S., Eigner Henke, K., Skop, V., Malinska, H., Trnovska, J., Kazdova, L., Drahota, Z., Mracek, T., and Houstek, J. (2016) Autocrine effects of transgenic resistin reduce palmitate and glucose oxidation in brown adipose tissue. *Physiol Genomics* 48, 420-427

68. Pejnovic, N. N., Pantic, J. M., Jovanovic, I. P., Radosavljevic, G. D., Milovanovic, M. Z., Nikolic, I. G., Zdravkovic, N. S., Djukic, A. L., Arsenijevic, N. N., and Lukic, M. L. (2013) Galectin-3 deficiency accelerates high-fat diet-induced obesity and amplifies inflammation in adipose tissue and pancreatic islets. *Diabetes* 62, 1932-1944

69. Pejnovic, N. N., Pantic, J. M., Jovanovic, I. P., Radosavljevic, G. D., Djukic, A., Arsenijevic, N. N., and Lukic, M. L. (2013) Galectin-3 is a regulator of metaflammation in adipose tissue and pancreatic islets. *Adipocyte* 2, 266-271

70. Weber, M., Sporrer, D., Weigert, J., Wanninger, J., Neumeier, M., Wurm, S., Stogbauer, F., Kopp, A., Bala, M., Schaffler, A., and Buechler, C. (2009) Adiponectin downregulates galectin-3 whose cellular form is elevated whereas its soluble form is reduced in type 2 diabetic monocytes. *FEBS Lett* 583, 3718-3724

71. Scatena, M., Liaw, L., and Giachelli, C. M. (2007) Osteopontin: a multifunctional molecule regulating chronic inflammation and vascular disease. *Arterioscler Thromb Vasc Biol* 27, 2302-2309

72. Kiefer, F. W., Zeyda, M., Todoric, J., Huber, J., Geyeregger, R., Weichhart, T., Aszmann, O., Ludvik, B., Silberhumer, G. R., Prager, G., and Stulnig, T. M. (2008) Osteopontin expression in human and murine obesity: extensive local up-regulation in adipose tissue but minimal systemic alterations. *Endocrinology* 149, 1350-1357

73. Kiefer, F. W., Zeyda, M., Gollinger, K., Pfau, B., Neuhofer, A., Weichhart, T., Saemann, M. D., Geyeregger, R., Schlederer, M., Kenner, L., and Stulnig, T. M. (2010) Neutralization of osteopontin inhibits obesity-induced inflammation and insulin resistance. *Diabetes* 59, 935-946

74. De Fusco, C., Messina, A., Monda, V., Viggiano, E., Moscatelli, F., Valenzano, A., Esposito, T., Sergio, C., Cibelli, G., Monda, M., and Messina, G. (2017) Osteopontin: Relation between Adipose Tissue and Bone Homeostasis. *Stem Cells International*

75. Lidell, M. E., and Enerback, S. (2015) Brown adipose tissue and bone. *Int J Obes Suppl* 5, S23-27

Footnotes

This work was funded by the EU FP7 Collaborative Project DIABAT (HEALTH-F2-2011-278373) and the Helmholtz Alliance ICEMED (HA-314).

Data Availability

The mass spectrometry proteomics data have been deposited to the ProteomeXchange Consortium (http://proteomecentral.proteomexchange.org) via the PRIDE (16) partner repository with the dataset identifier PXD009280. Annotated MS/MS spectra can be viewed through MS-Viewer (http://msviewer.ucsf.edu/prospector/cgi-bin/msform.cgi?form=msviewer) with the search key *2rncktsta6*.

Figure Legends

Figure 1: Principle and experimental design of the secretome analysis. The secretome analysis workflow started with incubation of primary white or brown adipocytes with media lacking methionine, lysine and arginine for 30 min followed by media supplemented with L-azidohomoalanine (AHA) and either intermediate or heavy isotope labeled amino acids (lysine and arginine) for 24 hours. In addition, 0.5 µM NE was added in selected analyses. After incubation, the supernatants were collected and the secreted (AHA-containing) proteins were enriched via click-chemistry, washed, digested, fractionated and analyzed by LC-MS/MS.

Figure 2: Comparative secretome analysis between primary murine white and brown adipocytes. A) Volcano plot depicting 141 significantly (p.adj < 0.05, nominal p-value cutoff = 0.023) differentially secreted proteins including 11 known adipokines (in green). B) GO enrichment analysis of the 141 proteins based on their higher secretion in white or brown adipocytes, with significantly enriched GO terms in color (p-value threshold of 0.01) and non-significant ones in grey (p-value threshold of 0.1). C) Volcano plot as in panel A. Proteins belonging to the enriched GO terms are named and colored. Additionally, the top differentially secreted proteins that are discussed in the results are labeled in black. WA: white adipocytes, BA: brown adipocytes.

Figure 3: Comparative secretome analysis between primary murine white and brown adipocytes upon NE stimulation. A) Volcano plot depicting 186 significantly (p.adj < 0.05, nominal p-value cutoff = 0.023)

differentially secreted proteins including 13 known adipokines (in green). B) GO enrichment analysis of the 186 proteins based on their higher secretion in white or brown adipocytes, with significantly enriched GO terms in color (p-value threshold of 0.01) and non-significant ones in grey (p-value threshold of 0.1). C) Volcano plot as in panel A. Proteins belonging to the enriched GO terms are named and colored. Additional top differentially secreted and discussed proteins are named in black. WA: white adipocytes, BA: brown adipocytes.

Figure 4: The secretory response of primary murine white and brown adipocytes between the NE-stimulated and basal state. Scatterplot representing the fold changes of the significantly differentially secreted proteins from figures 2 and 3, i.e. between white and brown adipocytes in the basal state and upon NE-stimulation. Proteins in Q1 and Q2 represent white adipocyte-enriched adipokines in the unstimulated state (y-axis > 0), while Q3 and Q4 display brown adipocyte-enriched adipokines in the basal state (y-axis < 0). Proteins in Q1 and Q4 are more secreted from white than brown adipocytes upon NE (x-axis > 0), while Q2 and Q3 represent proteins higher secreted from brown than white adipocytes upon NE (x-axis < 0). Only proteins that were detected in both analyses are represented. Proteins with preferential NE-responsive secretion in brown or white adipocytes are labeled in black. WA: white adipocytes, BA: brown adipocytes, Q1-4: quadrant 1-4.

Figure 5: Comparative secretome analysis of primary murine brown adipocytes with and without NE. A) Volcano plot depicting 280 significantly (p.adj < 0.05, nominal p-value cutoff = 0.023) differentially secreted proteins and 10 known adipokines (in green). B) GO enrichment analysis (p-value threshold of 0.01) of the 280 proteins based on their higher secretion with or without NE. Significantly enriched GO terms are in color and non-significant ones in grey (p-value threshold of 0.1). C) Volcano plot as in panel A. Proteins belonging to the enriched GO terms are colored, respectively. Additional top differentially secreted and discussed proteins are named in black. WA: white adipocytes, BA: brown adipocytes.

Figure 1

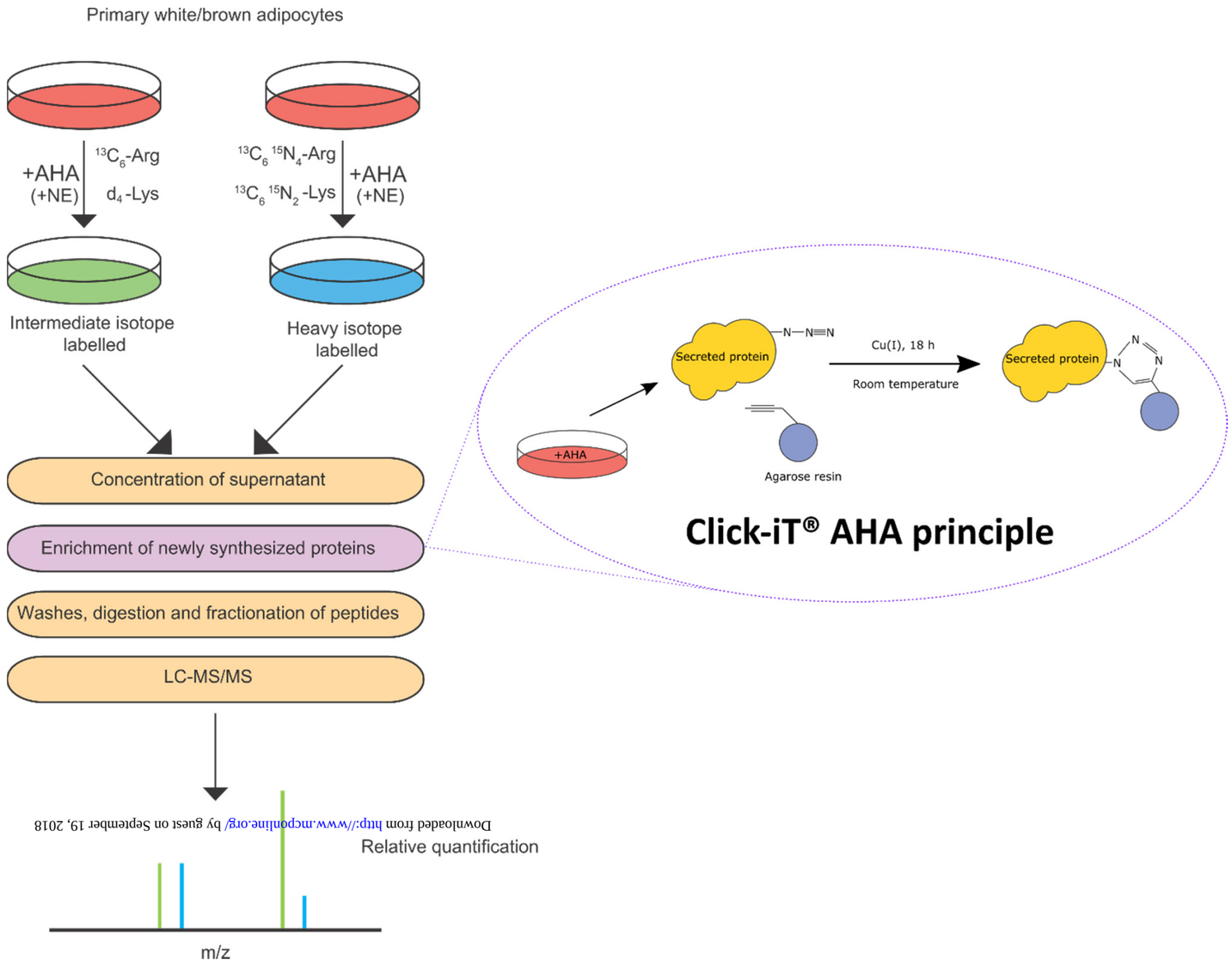

Figure 2

A

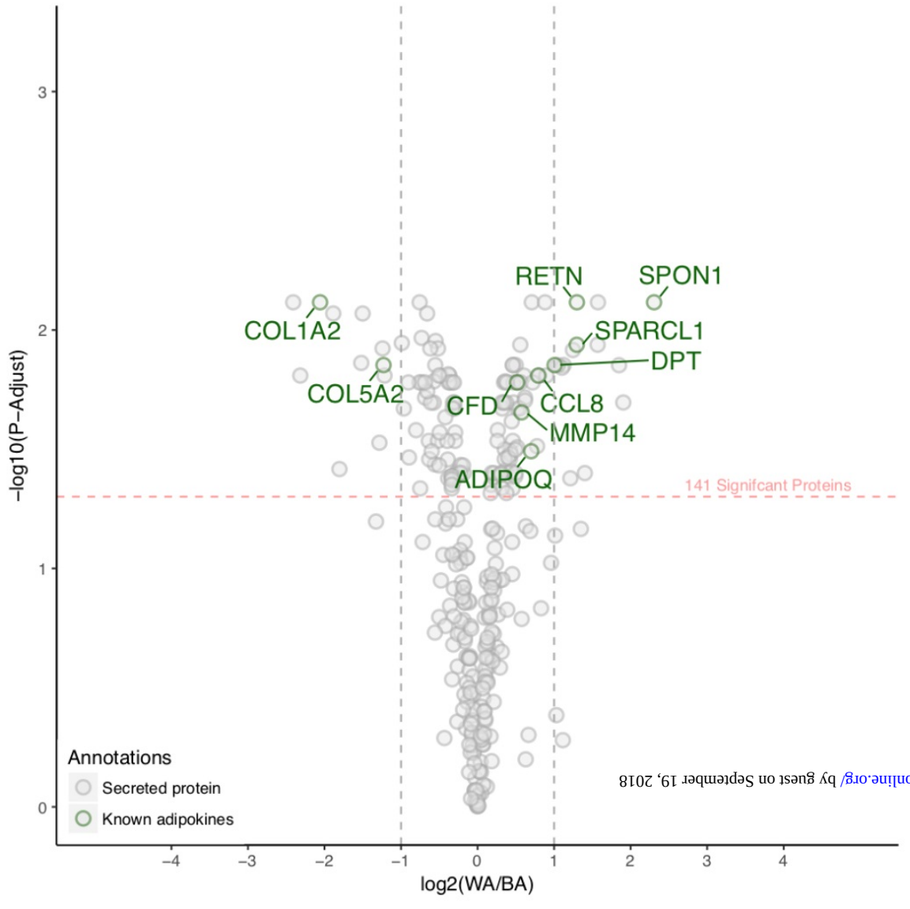

B

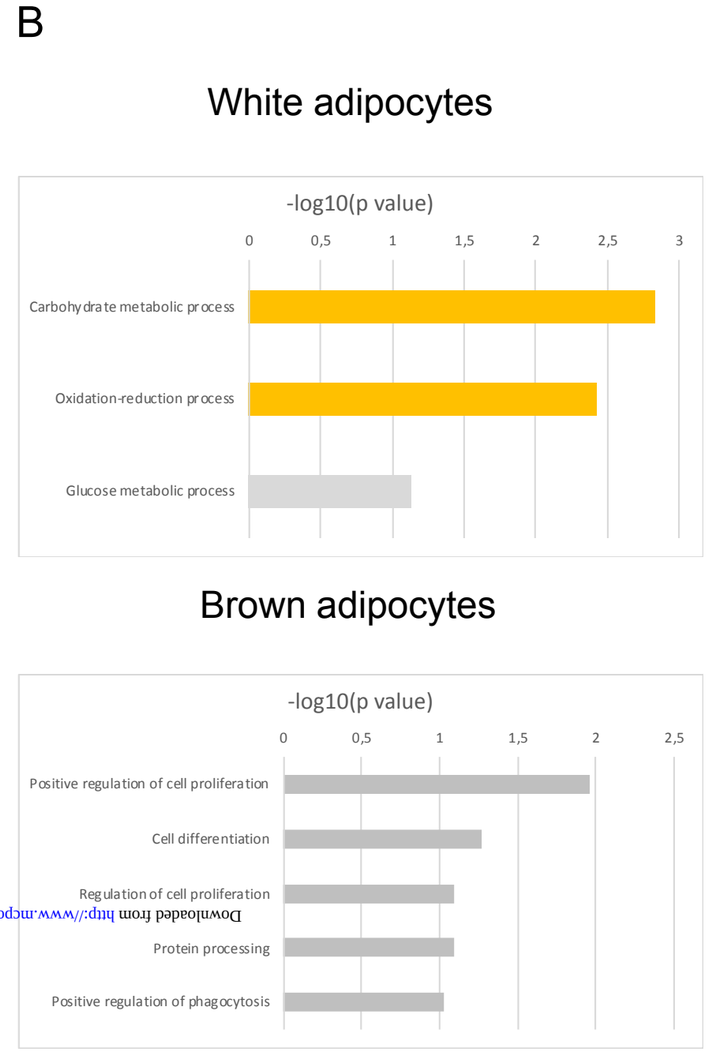

C

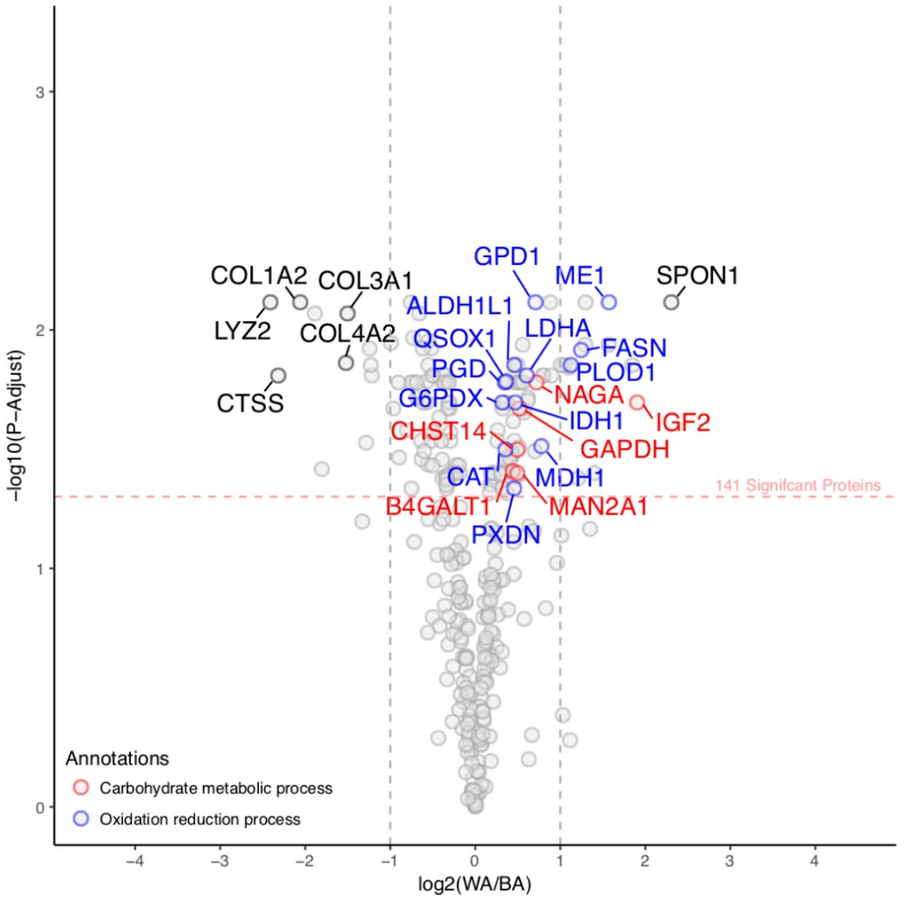

Figure 3

A

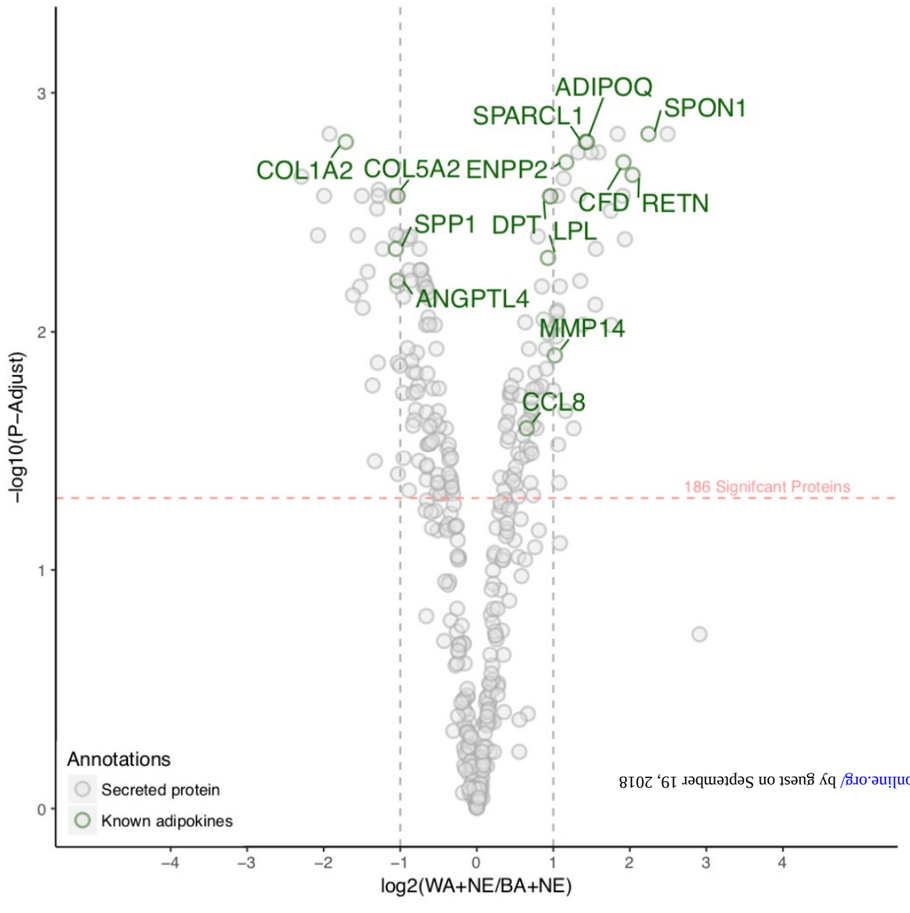

B

White adipocytes + NE

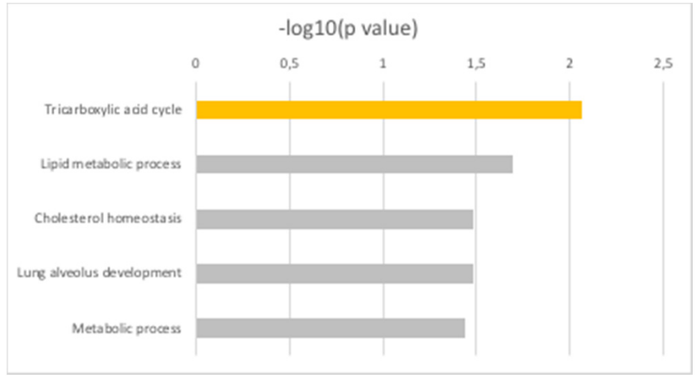

Brown adipocytes + NE

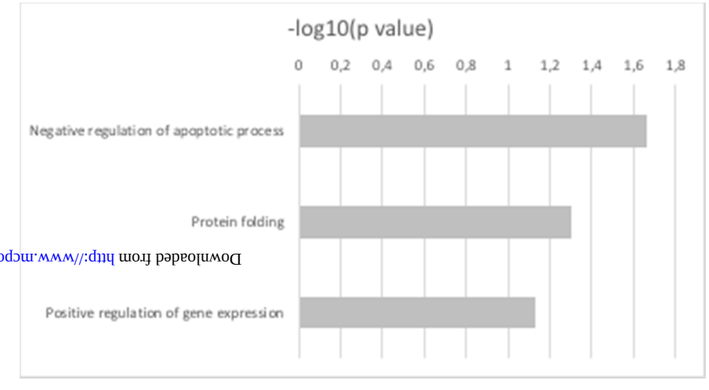

C

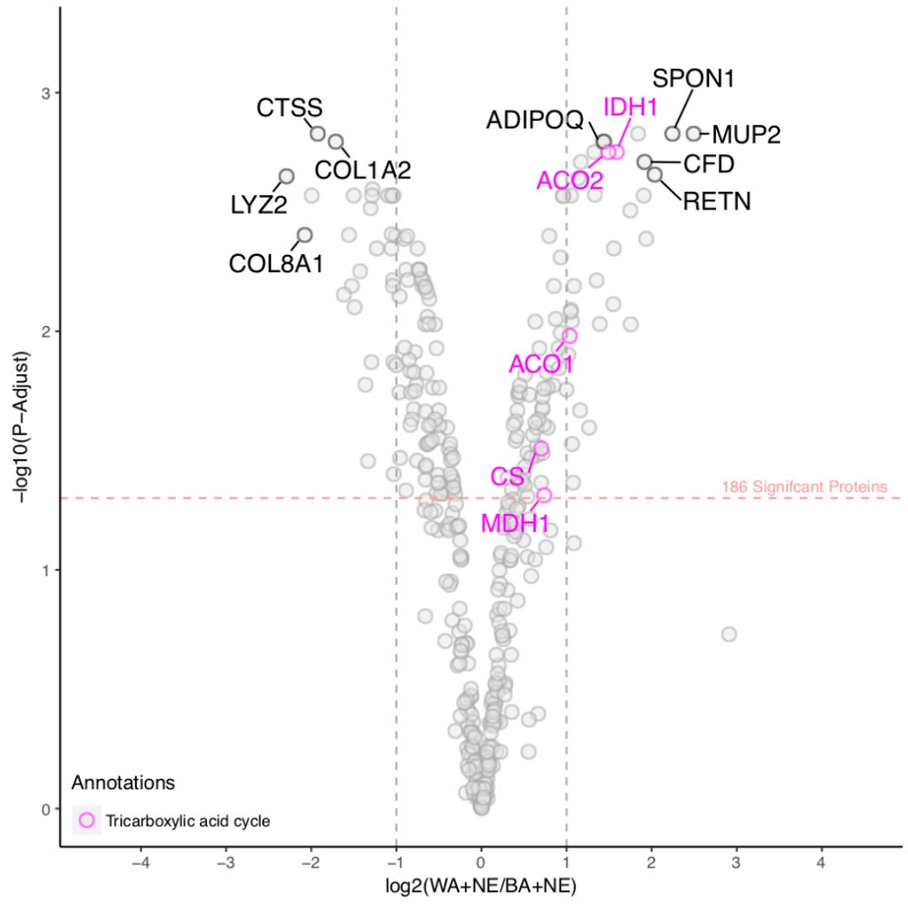

Figure 4

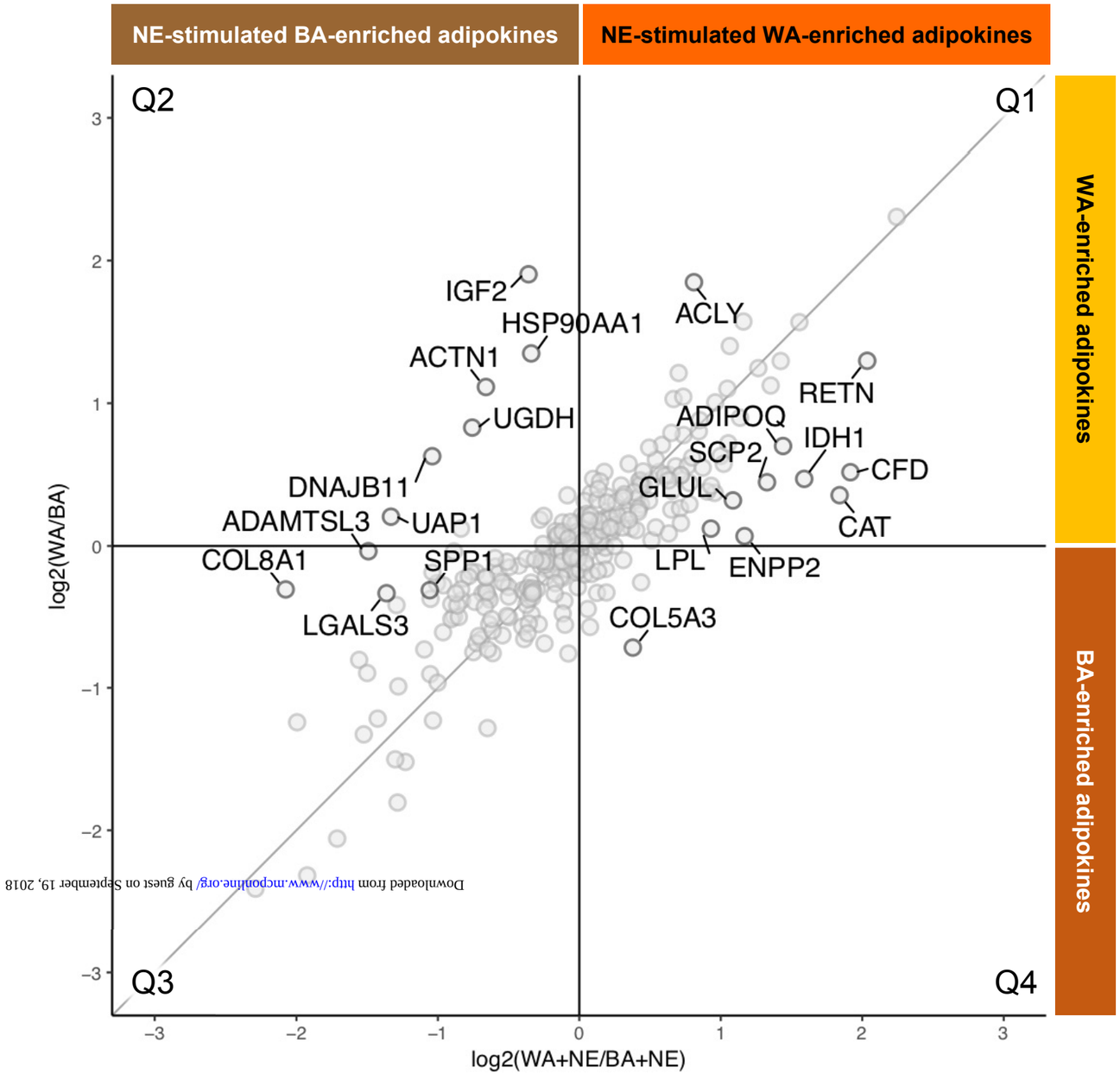

Figure 5

A

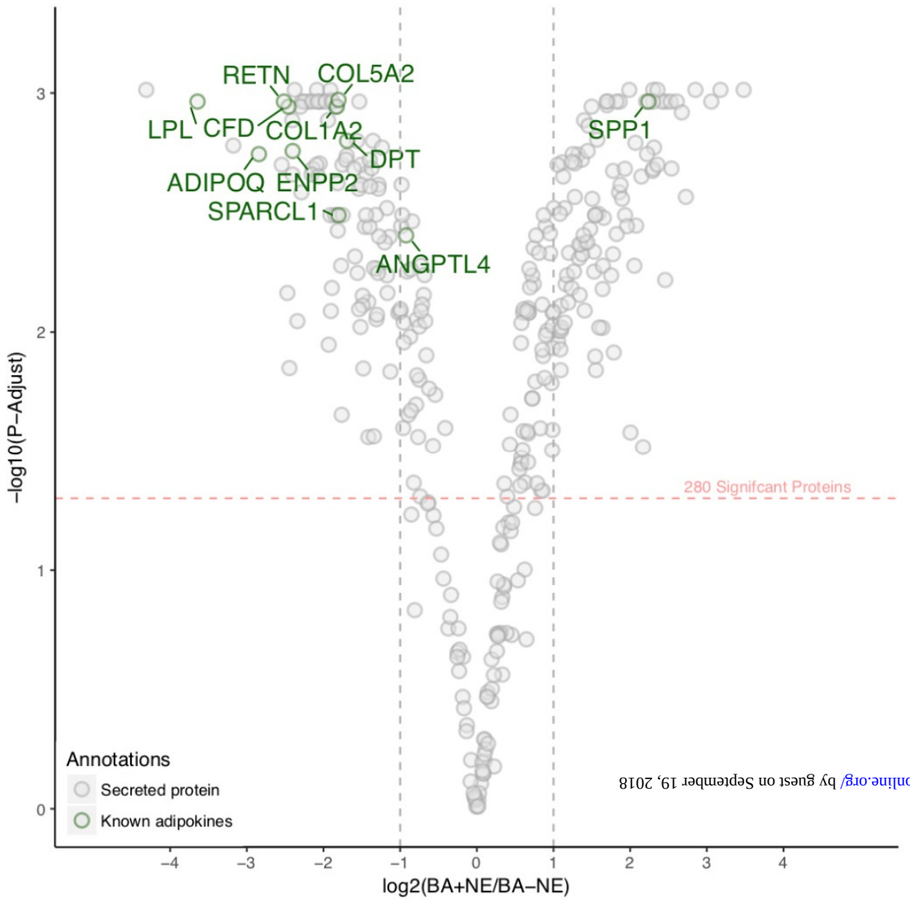

B

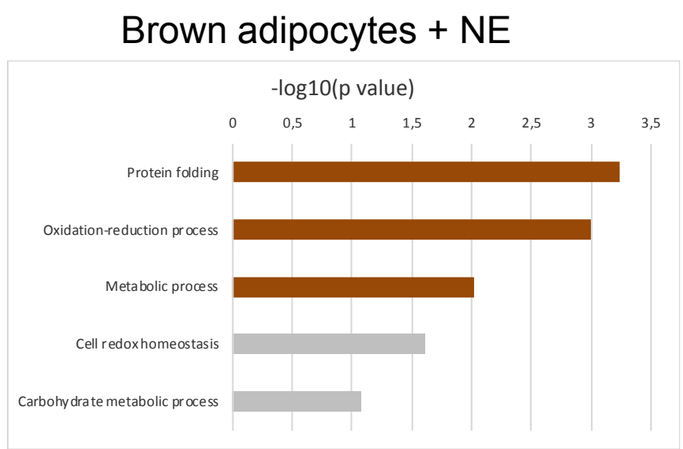

C